

Article

The Influence of Temperature on the Hydration Rate of Cements Based on Calorimetric Measurements

Włodzimierz Kiernożycki  and Jarosław Błyszko * 

Department of Reinforced Concrete Structures and Concrete Technology, Faculty of Civil and Environmental Engineering, West Pomeranian University of Technology in Szczecin, Aleja Piastów 50a, 70-311 Szczecin, Poland; Wlodzimierz.Kiernozycki@zut.edu.pl

* Correspondence: jaroslaw.blyszko@zut.edu.pl

Abstract: The study presents results of calorimetric tests of three different cements. Two Ordinary Portland cements, CEM I 52.5 R and CEM I 42.5 R, and one Blastfurnace cement, CEM III/A 42.5 N LH/HSR/NA, were analysed. The analysis has shown that the empirical formulas derived based on the results can successfully replace the Arrhenius formula in determination of the hydration rate in relation to curing temperature. It was proven that the hydration rate in relation to the curing temperature changes with the progression of hydration. The study introduces an E_n coefficient which determines the influence of curing temperature on generation of heat. Results of the study have shown that the value of E_n is not constant and changes with the progression of hydration process. Proposed method of numerical modelling of the total heat generated and generation rate based on obtained results allows for the calculation of those two parameters for any curing conditions.

Keywords: cement; isothermal calorimetry; heat of hydration; concrete maturity



Citation: Kiernożycki, W.; Błyszko, J. The Influence of Temperature on the Hydration Rate of Cements Based on Calorimetric Measurements. *Materials* **2021**, *14*, 3025. <https://doi.org/10.3390/ma14113025>

Academic Editor: Francisca Puertas

Received: 4 May 2021

Accepted: 26 May 2021

Published: 2 June 2021

Publisher's Note: MDPI stays neutral with regard to jurisdictional claims in published maps and institutional affiliations.



Copyright: © 2021 by the authors. Licensee MDPI, Basel, Switzerland. This article is an open access article distributed under the terms and conditions of the Creative Commons Attribution (CC BY) license (<https://creativecommons.org/licenses/by/4.0/>).

1. Introduction

Design of concrete constructions requires not only including the loads occurring during their service life but also the ones that can appear during the execution stage. Indirect loads generated by the hydration of cement-based materials and direct loads from execution processes are both present. Analysis of the after-effects of the indirect (thermal and shrinkage) and direct loads (dead loads) requires determining the influence of temperature on the hydration processes of concrete [1,2].

The heat generated by the hydration process during execution of concrete is the major cause of uneven heat distribution in massive elements [3]. Heat distribution and time of temperature equalization is influenced by different heat generation rates and total amount of generated heat. Thus, it is necessary to use admixtures for control of generated heat and to conduct tests to determine the heat generation rates of concrete. Based on initial test results, certain preventive actions are taken, including using low-heat cements, increasing aggregate content in the mix, conducting measurements of the temperature during execution or cooling with water [4]. In recent years, due to dynamic development of admixtures and FEM modelling, the issue of heat generation was studied by various authors [5–11].

The review of existing studies has shown different ways to describe the influence of curing temperature on the hydration rate of cement and corresponding strength development [12–17]. A.G. Saul [18] has proposed a time-temperature factor (TTF), also known as a maturity index, as a way to express the development of concrete's strength. Rastrup [19] has introduced an equivalent age concept based on the van't Hoff's chemical principle in which the rate of reaction doubles with the increase of temperature by 10 °C.

The issue of determining the equivalent maturing time in different temperatures was studied by many researchers [20–25]. Currently two procedures are used to determine the maturity of executed concrete in reference to standard curing temperature (20 °C).

These procedures are Standard Practice for Measuring Hydration Kinetics of Hydraulic Cementitious Mixtures Using Isothermal Calorimetry (ASTM C1679-08) [26] and Standard Practice for Estimating Concrete Strength by the Maturity Method (ASTM C1074_11) [27].

Both methods in their principle refer to Arrhenius equation, which, as opposed to both above mentioned propositions allows to include also the properties of used cement. The reserved attitude towards this approach results from use of the activation energy E . Kurdowski and Pichniarczyk [28] have objected to using the energy activation, that comes from the kinetic gas theory, for considerations of cement hydration.

Despite numerous studies [23,24,29–33], there is still no consensus on which approach and variables should be used for the purpose of maturity method (i.e., apparent activation energy).

The study presents the results of calorimetric tests of different cements under various maturing conditions. Results of the study allowed for the proposal of a method for describing the influence of curing temperature on heat generation of studied cements. Empirical formulas that include the influence of physicochemical properties of cements for the studied range of temperatures were proposed. To correlate the results acquired for the reference temperature of 20 °C, the study introduces an E_n coefficient for each of studied cements. The proposed approach showed good correlation of the results.

2. Materials and Methods

2.1. Materials

For the purpose of this study, three different types of cement were chosen: Ordinary Portland Cement CEM I 52.5 R, CEM I 42.5 R and Blastfurnace Cement CEM III/A 42.5 N-LH/HSR/NA (CEM III 42.5 N), all manufactured by Góraźdże Cement in Chorula, Poland. Cement characteristics are given in Table 1.

Table 1. Properties of cements used in the study.

Characteristic	CEM I 52.5 R	CEM I 42.5 R	CEM III 42.5 N
Composition [%]			
Portland clinker	95 ÷ 100	95 ÷ 100	35 ÷ 64
Ground granulated blast furnace slag	-	-	36 ÷ 65
Secondary components	0 ÷ 5	0 ÷ 5	0 ÷ 5
Compressive strength [MPa]			
2 days	36.2	29.0	14.8
28 days	63.6	56.9	58.3
Setting time (initial) [min]	170	184	201
Surface area (Blaine) [cm ² /g]	4411	3717	4636
Chemical composition [%]			
SO ₃	2.93	2.93	2.70
Cl ⁻	0.067	0.066	0.080
Loss on ignition	3.73	3.40	1.08
Insoluble residue	0.72	0.70	0.48
Heat of hydration (7 days) [J/g]	325 ÷ 375	325 ÷ 375	<270

The amount of gypsum in studied cements was <5% as required by European Standards.

2.2. Test Procedure

Heat of hydration and heat flow was determined in a three-channel isothermal calorimeter TAM AIR by TA Instruments (New Castle, DE, USA). The dual-channel system allows one to test simultaneously cement specimen and reference specimen. The software allows one to measure the heat in extended periods with a measuring error of ±0.02 °C. Test specimen and the equipment were prepared in accordance to EN 196-11 [34].

Cement paste specimen with a water–cement ratio of 0.5 was used in the study. After acquiring base temperature by the paste components and calorimeter, the specimens were prepared. Water (15 g) was added to cement (30 g) and mixed for 60 s by hand in a container used for calorimeter. The container was insulated with a cloth to block the heat coming from hand. The container was immediately placed into the calorimeter with base line prepared. Time between adding water to first measurement did not exceed 2 min. The reference specimen was prepared by replacing the cement with a silica sand. Directly after mixing, the samples were set on a 7-day long cycle where generated heat and heat flow were measured. The study was performed for different curing temperatures of 20 °C, 25 °C, 30 °C and 40 °C.

3. Results

Results of generated heat and heat flow for different cements are presented in Figures 1 and 2 and Table 2.

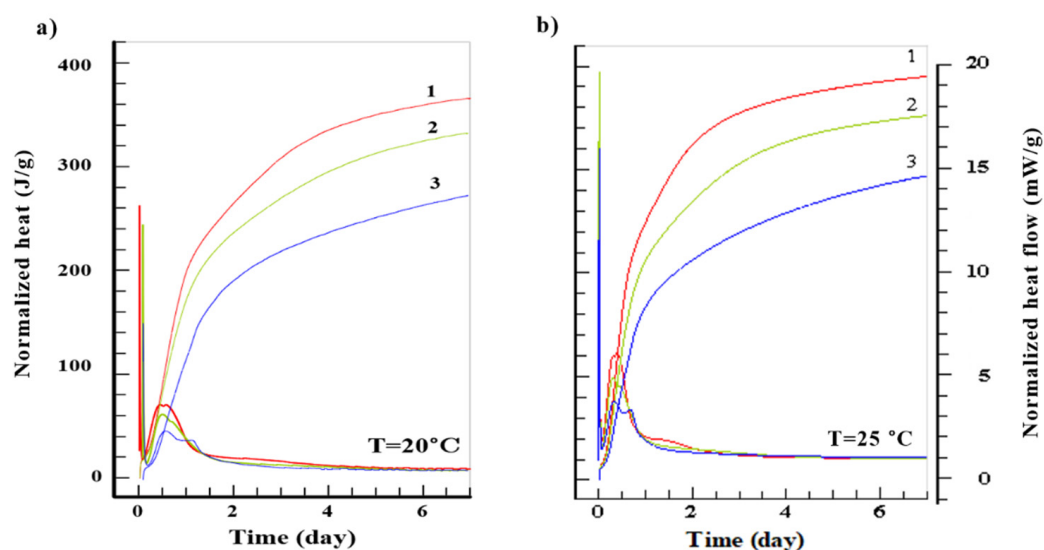


Figure 1. Amount of generated heat (J/g) and heat flow (mW/g) of studied cements: 1. CEM I 52.5 R, 2. CEM I 42.5 R, 3. CEM III 42.5 N for curing temperatures 20 °C (a) 25 °C (b).

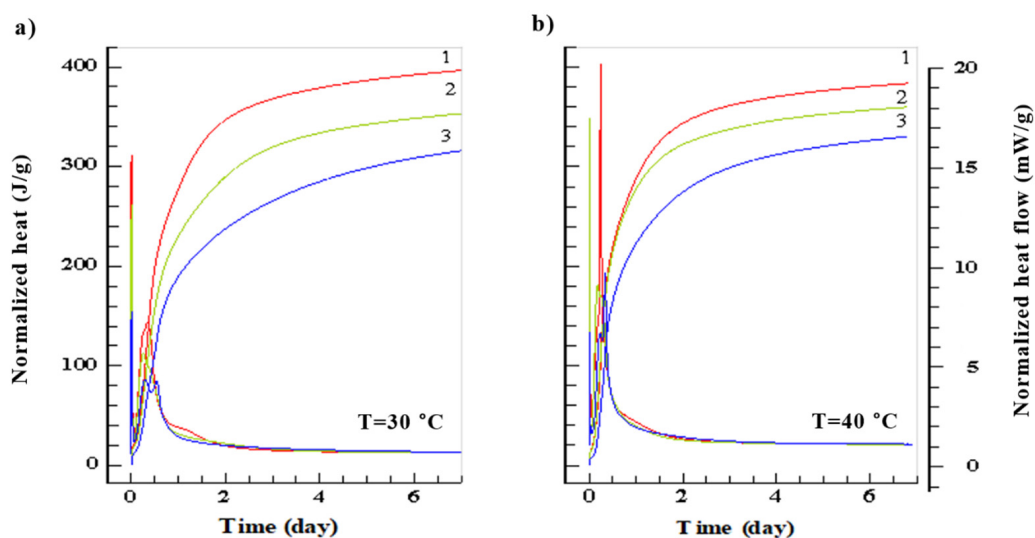


Figure 2. Amount of generated heat (J/g) and flow (mW/g) of studied cements: 1. CEM I 52.5 R, 2. CEM I 42.5 R, 3. CEM III 42.5 N for curing temperatures 30 °C (a) 40 °C (b).

Table 2. Results of calorimetric tests for studied cements.

Cement	Temperature (°C)	Q_7 ¹ (J/g)	max. $dQ/d\tau$ (mW/g)	τ_{\max} ³ (h, min)
CEM I 52.5 R	20	366	3.06	12 h 5 min
	25	390	5.10	8 h 50 min
	30	396	6.38	7 h 45 min
	40	384	19.17	5 h 50 min
CEM I 42.5 R	20	332	2.66	10 h 45 min
	25	352	3.92	7 h 50 min
	30	353	4.91	6 h 10 min
	40	360	7.90	4 h 10 min
CEM III 42.5 N	20	272	1.93	11 h 25 min
	25	294	2.77	8 h 55 min
	30	316	3.59	7 h 30 min
	40	330	8.64	8 h 15 min

¹ Q_7 —Heat of hydration. ² Maximum value of normalized heat. ³ Time in which $dQ/d\tau$ reaches maximum, h (hours), min (minutes).

After 7 days of maturing the highest normalized heat of hydration, regardless of the curing temperature, was generated by the CEM I 52.5 R ($Q_7 = 366 \div 396$ J/g), and the lowest was generated by CEM III 42.5 N ($Q_7 = 272 \div 330$ J/g). Heat flow was again the highest for CEM I 52.5 R ($dQ/d\tau = 3.06 \div 19.17$ mW/g), while the lowest for CEM III 42.5 N ($dQ/d\tau = 1.93 \div 8.64$ mW/g). With the increase of the curing temperature the maximum heat flow $dQ/d\tau$ also increases. However, this does not correspond to highest total heat generated throughout the whole cycle. Detailed results of heat flow and total heat generated are presented in Table 2.

Initial rapid increase in heat generation (first peak) is caused by the absorption of water by the cement grains and chemical reaction on their surface. The second peak is caused by the intensified formation of the C-S-H gel, AF_t phase and CH. Of importance is also production of the $3CaO \cdot Al_2O_3$ and $4CaO \cdot 3Al_2O_3 \cdot SO_4$ which limits the hydration of C_3A [35]. With the increase of the surface area of cement and curing temperature, the heat generation rate also increases. The third peak clearly visible in case of the blastfurnace cement, especially for higher curing temperatures, is caused by the activation of the slag by the $Ca(OH)_2$ and SO_4^{2-} ions [36]. This additional peak, found sometimes in other cements at the end of the 4th stage of hydration [37], is caused by the hydration of remaining C_3A and creation of hexagonal aluminates.

4. Discussion

Results presented in this study do not allow one to directly correlate the influence of curing temperature on the maturing of specimen. To determine the correlation, the following equation was introduced (1):

$$v = A_0 \exp\left(-\frac{E_n}{T}\right), \quad (1)$$

in which the reaction rate v is expressed as an exponential function of E_n constant and curing temperature T in Celsius degrees. The constants A_0 and E_n can be determined based on the experimental results of reaction rate v in different curing conditions. Equation (1) can be transformed to:

$$\ln v = \ln A_0 - \frac{E_n}{T} = B - \frac{E_n}{T} \quad (2)$$

where the temperature T is expressed in Celsius and E_n determines the influence of temperature on heat generation. The $\ln v = f(1/T)$ graph of (2) shows linear function with a slope of $tg\alpha = E_n$.

To determine the E_n in accordance to (2), results presented in Figure 1 were transformed into:

$$\frac{dQ(T)}{d\tau} = f(Q), \quad (3)$$

in which the T stands for different temperatures of maturing. Equation (3) determines the heat flow of cement under different curing temperatures at a given time as a total generated heat Q . The analysis for test specimen is presented in Figures 3–5. The E_n was determined for different levels of heat generated: $Q = 50 \text{ J/g}$, $Q = 100 \text{ J/g}$, $Q = 150 \text{ J/g}$, $Q = 200 \text{ J/g}$ and $Q = 250 \text{ J/g}$. Based on presented results, the slope of function (2) changes in time and depends on the hydration process stage. Biggest differences are observable in the first stage of hydration for the range of $Q = 50 \div 150 \text{ J/g}$. In later stages the lines are almost parallel, meaning that the values of E_n are similar. In Figures 3–5, the mean value from all of the measurements was marked with a black dotted line.

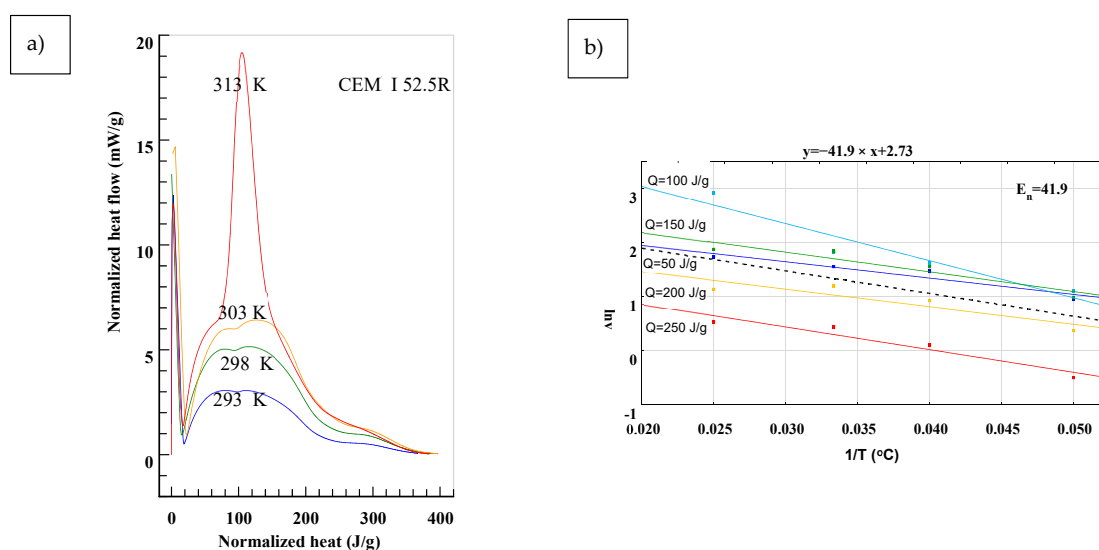


Figure 3. Determination of the E_n from the Equation (2) for CEM I 52.5 R. (a) Normalized heat flow in comparison to total heat generated for different temperatures, (b) Values of E_n for different temperatures and it's representative value calculated using least-square method.

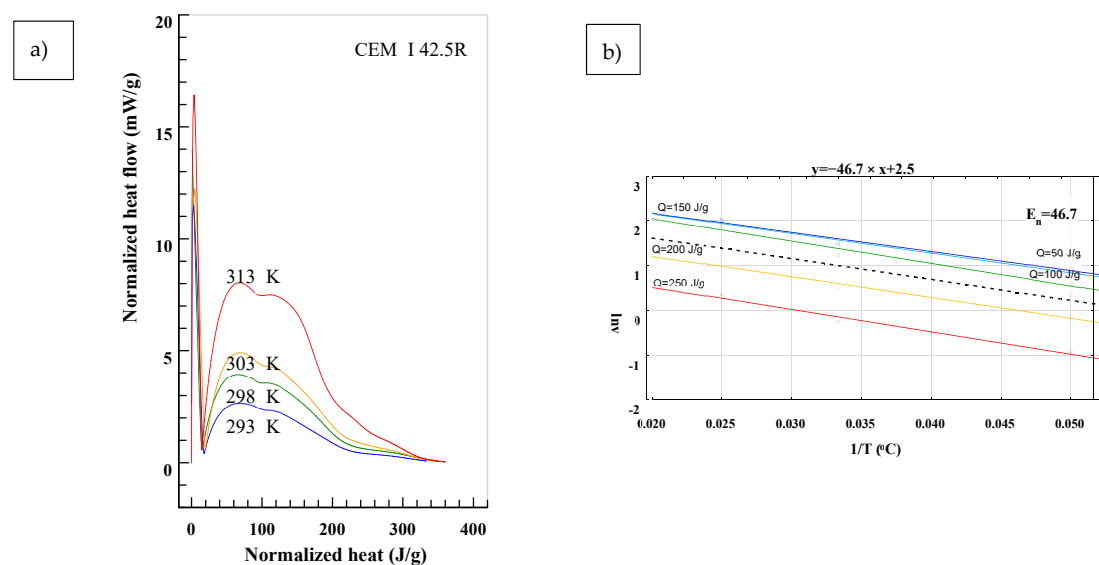


Figure 4. Determination of the E_n from the Equation (2) for CEM I 42.5 R. (a) Normalized heat flow in comparison to total heat generated for different temperatures, (b) Values of E_n for different temperatures and it's representative value calculated using least-square method.

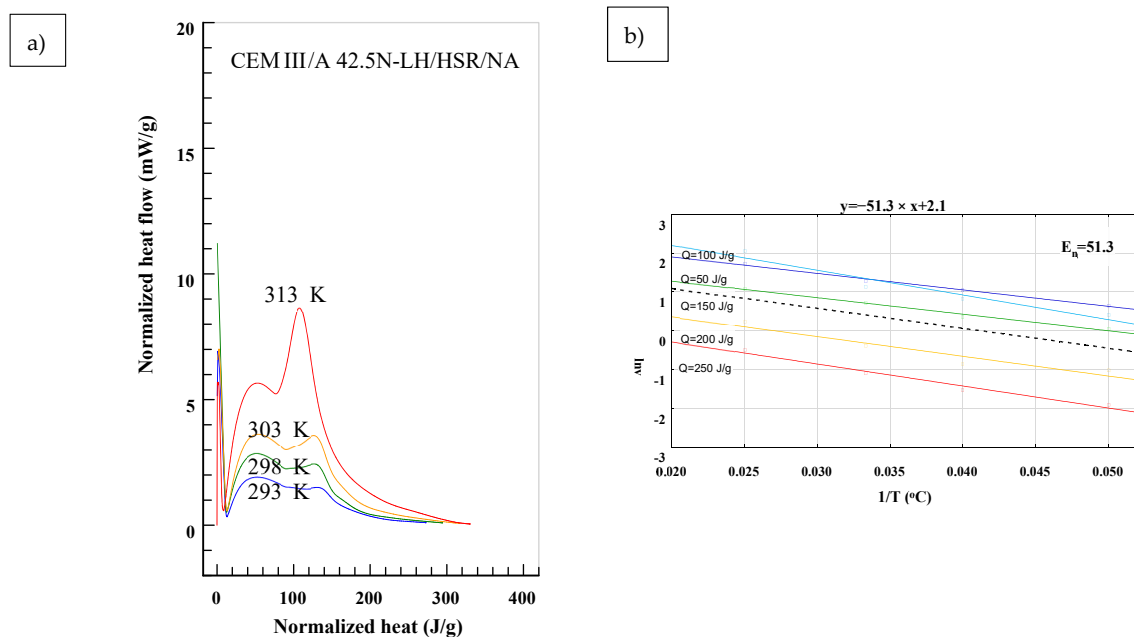


Figure 5. Determination of the E_n from the Equation (2) CEM III 42.5 N. (a) Normalized heat flow in comparison to total heat generated for different temperatures, (b) Values of E_n for different temperatures and its representative value calculated using least-square method.

Figure 6 presents the values of the E_n in relation to the level of total heat generated Q : 50, 100, 150, 200 and 250 J/g.

Results of the study have shown that the value of the E_n is not constant. The value of E_n changes with the progression of hydration process, which can be related to changes in the processes responsible for its rate. Performed tests have shown that after generating 100 J/g of heat, CEM I 52.5 R and CEM IIIA 42.5 N have higher values than the CEM I 42.5 R of the E_n parameter (respectively $E_n = 68.8$ and $E_n = 63.7$ to $E_n = 44.1$). In the opinion of the authors, this is probably caused by the higher surface area of two former cements equal to $4411 \text{ cm}^2/\text{g}$ and $4636 \text{ cm}^2/\text{g}$ compared to $3717 \text{ cm}^2/\text{g}$ for CEM I 42.5 R. It is worth mentioning that the maximum values of E_n occur when the heat flux $dQ/d\tau$ is also the highest.

To determine the susceptibility of studied cements to changes in temperature during hydration, it is better to refer to the mean value of the E_n . Results presented in Figure 5 allowed one to draw a conclusion that CEM I 52.5 R, with the highest strength, has the lowest value of $E_n = 41.9$, meaning its susceptibility to temperature changes is the lowest.

The blastfurnace cement has the highest value of $E_n = 51.3$ in this study, meaning it is the most susceptible to temperature changes from all studied cements. It was observed that the CEM I 42.5 with the highest surface area had the most linear $E_n = f(Q)$ function and $E_n = 46.7$. The statement was rephrased. When comparing the results of conducted tests to data presented in Table 1, it can be noticed that the hydration heat and susceptibility to curing temperature is different between the cements. Analysis of the thermal stresses caused by the hydration heat in mass construction should be made taking into consideration detailed data on the hydration heat and heat flux for used cement.

Figure 7 presents an example of temperature influence calculated based on (4) on the equivalent time t_e of CEM I 52.5 R in different temperatures. Based on the results it can be said that the maturing time $t = 100$ h in $T = 40$ °C equals equivalent time $t_e = 300$ h in $T_a = 20$ °C.

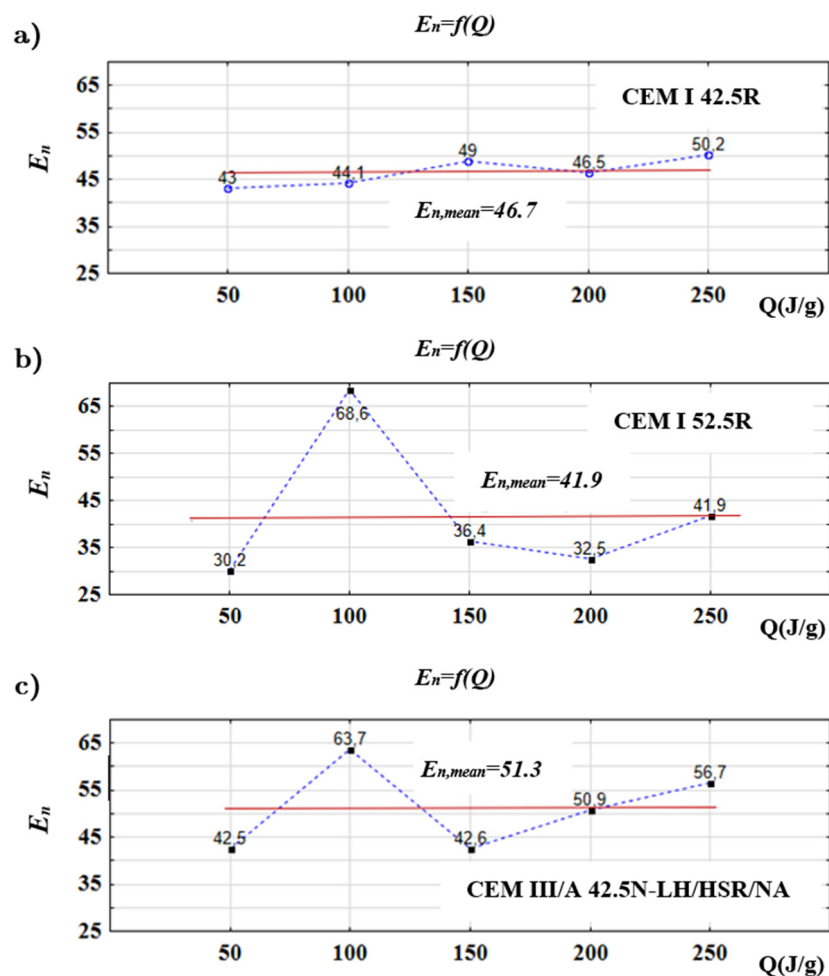


Figure 6. Values of the E_n in relation to the total heat generated Q calculated for studied cements (a) CEM I 52.5 R, (b) CEM I 42.5 R, (c) CEM III A 42.5 N.

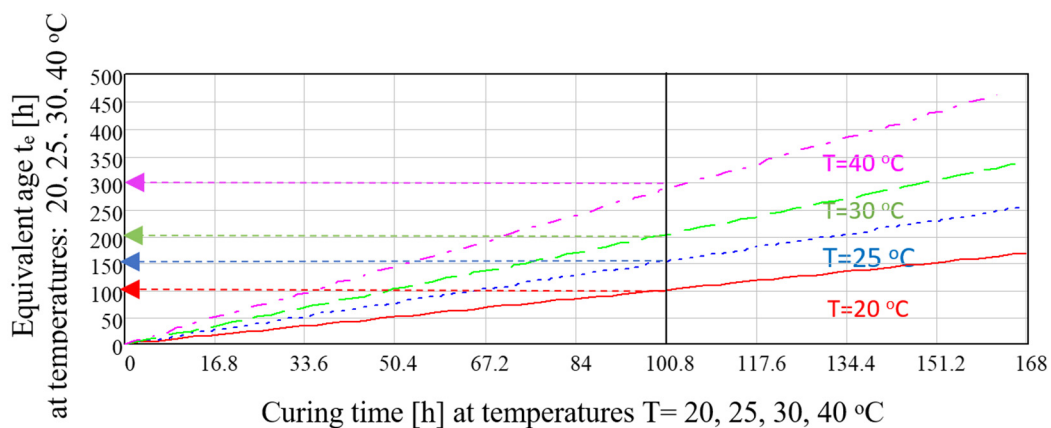


Figure 7. Equivalent age t_e for CEM I 52.5 R ($E_n = 41.9$) and different curing temperatures.

By analysing the influence of temperature T on the amount of generated heat of hydration $Q(T, t_e) = Q(T_a, t)$ based on (1), the equivalent time was derived $t_e = f(t)$:

$$t_e = \exp \left[-\frac{E_n}{T} \left(\frac{T_a - T}{T_a} \right) \right] t \tag{4}$$

Figure 8 presents the heat generated by hydration of studied cements in $T = 20, 25, 30$ i $40\text{ }^{\circ}\text{C}$ as a function of equivalent time t_e calculated with (5). The equivalent time t_e expressed by (5) and derived from (1) allows one to transform the results of the generated heat of hydration Q in reference temperature T_a to expect values of generated heat in any given temperature T . Numerical modelling of the hydration processes has a great significance in analysing the indirect load caused by the heat of hydration kinetics, particularly in mass concretes.

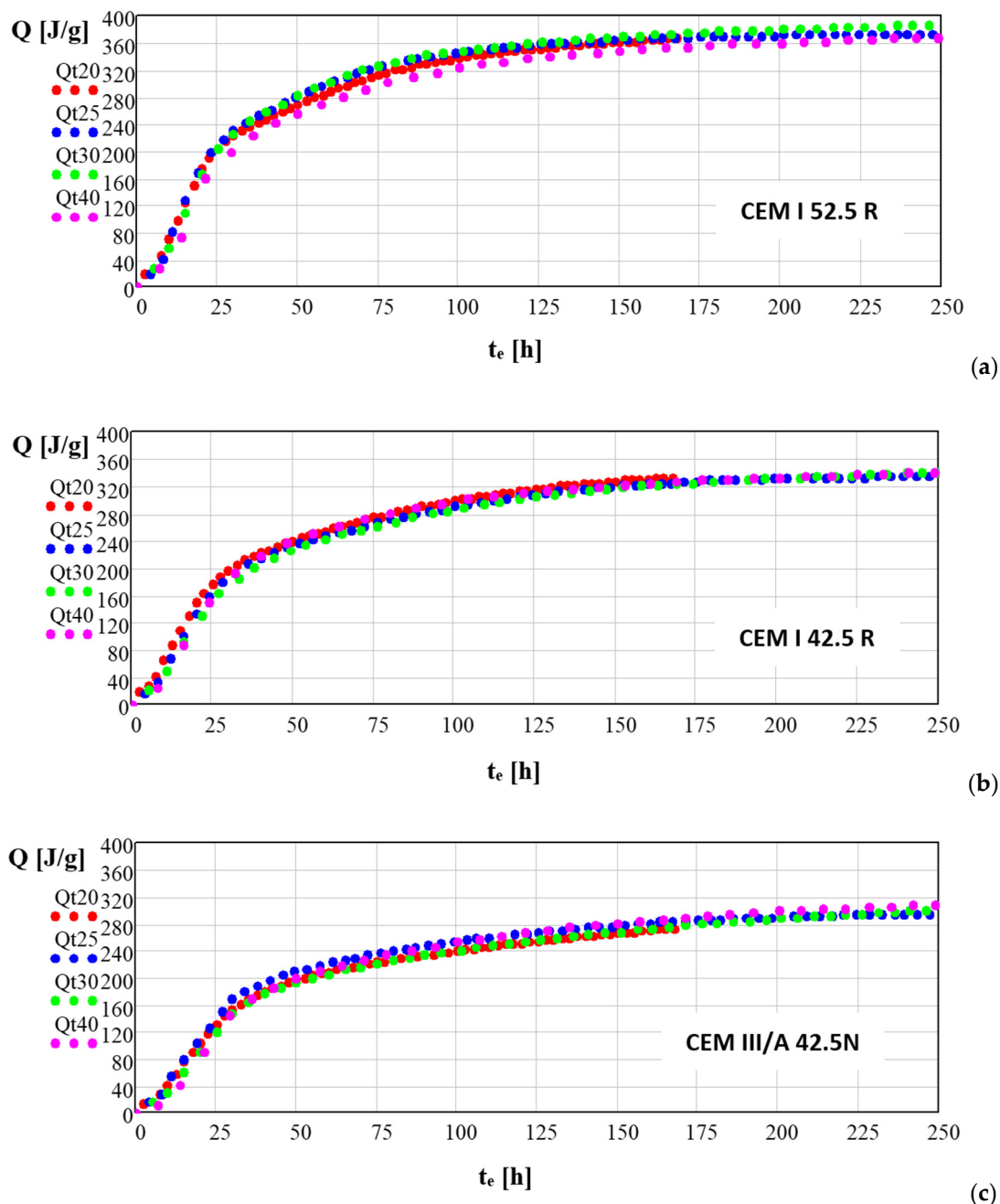


Figure 8. Generated heat Q (J/g) for studied cements in equivalent time function at curing temperatures of 20, 25, 30 and $40\text{ }^{\circ}\text{C}$. calculated for studied cements (a) CEM I 52.5 R, (b) CEM I 42.5 R, (c) CEM III A 42.5 N.

Many experimental numerical models calculate the development of hydration in relation to its chemical composition, surface area, water–cement ratio, internal pressure or maturing temperature. Validation of those models is typically based on calorimetric measurements. As the number of characteristics influences the heat of hydration in ce-

mentitious materials, determination of which of them has the greatest influence requires extensive testing [38]. Several studies proposed simpler modelling methods with parameters assumed for particular cement types which were determined in experimental tests.

Among those studies presented in [39], the model proposed by Wesche [40] seems particularly interesting. The heat of hydration of different cements is calculated as:

$$Q_t = Q \cdot \exp\left(P_1 \cdot t^{P_2}\right), \quad (5)$$

where Q is the heat of hydration, P_1 i P_2 are the parameters related to class and type of cement and t is the time of hydration. The function (5) works in a range of t ($t \rightarrow 0^+$, ∞) assuming values between $0 \div Q$. The derivative of the function (6):

$$\frac{dQ}{dt} = W_t = Q_t \cdot P_1 \cdot P_2 \cdot t^{(P_2-1)}, \quad (6)$$

assumes values of $W_t = 0$ at $t \rightarrow 0^+$ and $t = \infty$, and reaches its peak also in this range. Wesche has estimated the mean values of the P_1 and P_2 for higher class cements (in accordance to DIN standards): Z 55 ($P_1 = -11.1$ i $P_2 = -1.0$) and Z 25 L ($P_1 = -74.8$ i $P_2 = -1.5$).

Further analysis of the kinetics of hydration processes of studied cements in various temperatures was made using transformed (5) in which the absolute hydration time t was replaced by the equivalent time t_e , including the induction time t_i .

The estimation of unknown parameters of Equation (5) for all three studied cements and reference temperatures allowed for the derivation of the following formulas:

For CEM I 52.5:

$$Q_{o20(t)} = 353 \cdot \exp\left(-21.4 \cdot (t - 1.5)^{-0.94}\right) \quad (t_i = 1.5 \text{ h} \quad E_n = 41.9) \quad (7)$$

For CEM I 42.5 R:

$$Q_{o20(t)} = 345 \cdot \exp\left(-16.0 \cdot (t - 1.5)^{-0.97}\right) \quad (t_i = 1.5 \text{ h} \quad E_n = 46.7) \quad (8)$$

For CEM III/A-42.5N:

$$Q_{o20(t)} = 305 \cdot \exp\left(-9.7 \cdot (t - 3.0)^{-0.77}\right) \quad (t_i = 3.0 \text{ h} \quad E_n = 51.3) \quad (9)$$

Figure 9a presents an example of comparison between experimental results of heat generation Q_{e20} and results of W_{e20} calculated using (7) for CEM I 52.5 R and reference time $T_o = T = 20$ °C. Figure 9b shows the experimental results for temperature of 40 °C (Q_{e40} i W_{e40}) in comparison to results modelled using (4) and $T_o = 20$ °C and $T = 40$ °C.

Similar analysis was performed for blastfurnace slag, results of which are presented in Figure 10.

Relatively good compliance of the test results and calculated model was acquired in the study. Presented simple method of numerical modelling of generated heat of hydration and heat flow for determined influence of temperature E_n allows for the transformation of the reference results to any given hydration conditions. The concept, however, requires further studies for different cement pastes and concretes cured in isometrical and adiabatic conditions.

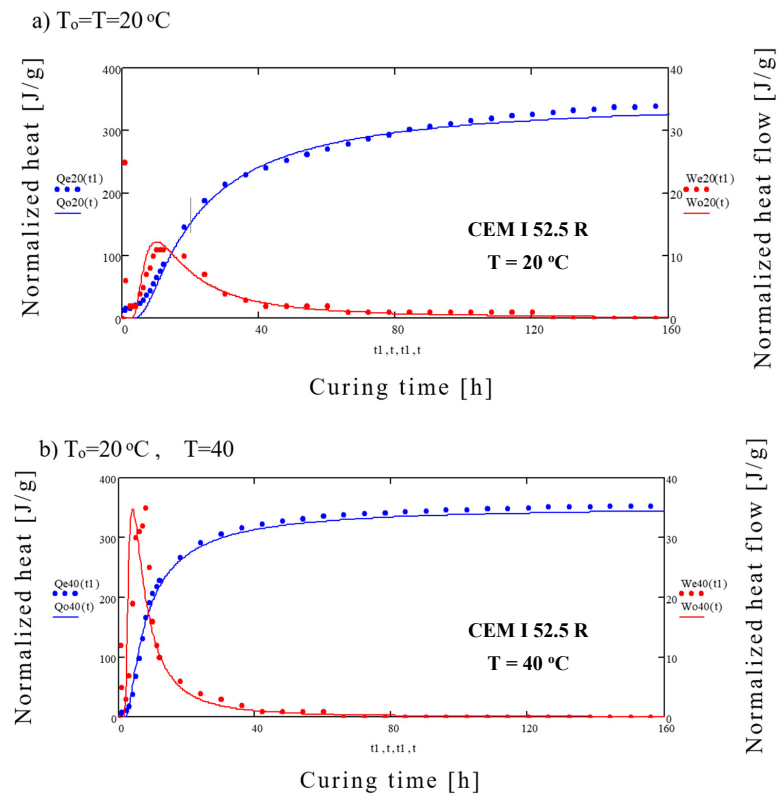


Figure 9. Comparison of experimental and calculated results of normalized heat and heat flow for the CEM I 52.5 R cement (a) for $T = 20\text{ }^\circ\text{C}$, (b) for $T = 40\text{ }^\circ\text{C}$.

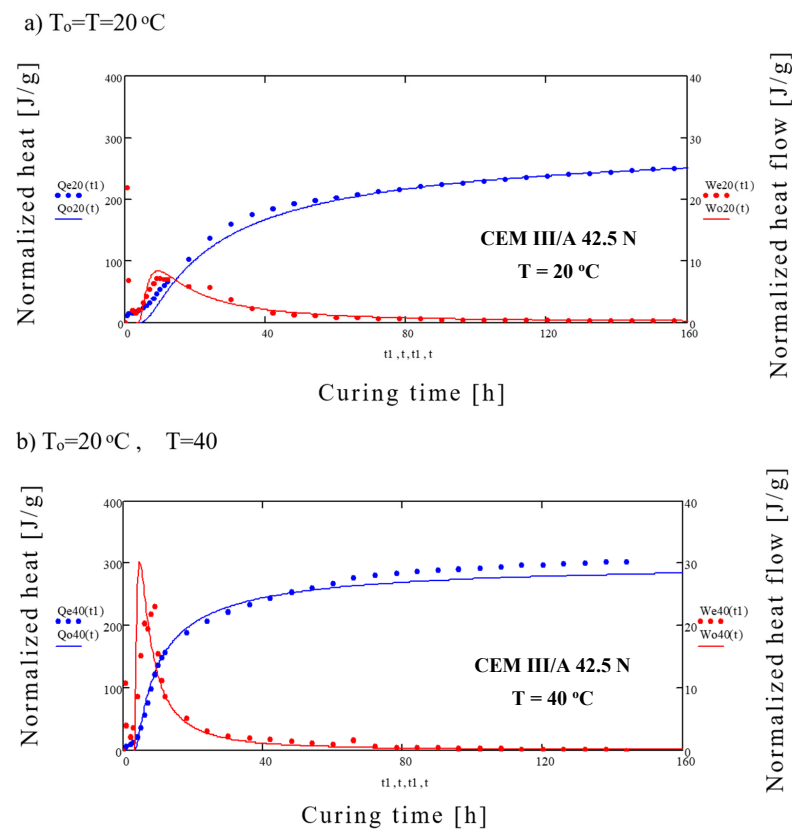


Figure 10. Comparison of experimental and calculated results of normalized heat and heat flow for the CEM III/A 42.5 N cement (a) for $T = 20\text{ }^\circ\text{C}$, (b) for $T = 40\text{ }^\circ\text{C}$.

5. Conclusions

The conducted tests performed on three different types of cements have shown that replacing classic Arrhenius formula with empirical equations that take into account the influence of curing temperature on hydration heat can provide good evaluation of susceptibility of those cements to temperature changes. Results of this study have shown that the susceptibility of cement to thermal conditions changes with the development of hydration process. Mean values of the susceptibility parameter determined for the first 7 days of hydration vary for different cement class and type. The presented simplified method of numerical modelling of heat generation and generation rate for determined value of the E_n parameter (influence of curing temperature on cement hydration) allows for the recalculation of the results acquired in reference conditions for any given temperature.

Author Contributions: Conceptualization, W.K. and J.B.; methodology, W.K. and J.B.; validation, W.K.; formal analysis, W.K.; investigation, J.B.; resources, W.K. and J.B.; data curation, W.K. and J.B.; writing—original draft preparation, W.K.; writing—review and editing, J.B.; visualization, W.K. and J.B.; supervision, W.K. All authors have read and agreed to the published version of the manuscript.

Funding: This research received no external funding.

Institutional Review Board Statement: Not applicable.

Informed Consent Statement: Not applicable.

Data Availability Statement: Data available on request due to file type and size.

Conflicts of Interest: The funders had no role in the design of the study; in the collection, analyses, or interpretation of data; in the writing of the manuscript, or in the decision to publish the results.

References

- Nasir, M.; Baghabra Al-Amoudi, O.S.; Maslehuddin, M. Effect of placement temperature and curing method on plastic shrinkage of plain and pozzolanic cement concretes under hot weather. *Constr. Build. Mater.* **2017**, *152*, 943–953. [[CrossRef](#)]
- Klemczak, B.; Żmij, A. Insight into Thermal Stress Distribution and Required Reinforcement Reducing Early-Age Cracking in Mass Foundation Slabs. *Materials* **2021**, *14*, 477. [[CrossRef](#)]
- Chu, I.; Lee, Y.; Amin, M.N.; Jang, B.-S.; Kim, J.-K. Application of a thermal stress device for the prediction of stresses due to hydration heat in mass concrete structure. *Constr. Build. Mater.* **2013**, *45*, 192–198. [[CrossRef](#)]
- Batog, M.; Giergiczny, Z. Influence of mass concrete constituents on its properties. *Constr. Build. Mater.* **2017**, *146*, 221–230. [[CrossRef](#)]
- Su, J.; Zuo, G.W.; Li, W. Temperature Control Technique and Analysis of Mass Concrete in the Pile Cap of Main Pier in Yangtze River Bridge. *Dev. Ind. Manuf.* **2014**, *587–589*, 1407–1411. [[CrossRef](#)]
- Lee, M.H.; Chae, Y.S.; Khil, B.S.; Yun, H.D. Influence of Casting Temperature on the Heat of Hydration in Mass Concrete Foundation with Ternary Cements. *Dev. Ind. Manuf.* **2014**, *525*, 478–481. [[CrossRef](#)]
- Xu, W.; Qiang, S.; Hu, Z.; Ding, B.; Yang, B. Effect of Hydration Heat Inhibitor on Thermal Stress of Hydraulic Structures with Different Thicknesses. *Adv. Civ. Eng.* **2020**, *2020*, 5029865. [[CrossRef](#)]
- Ju, Y.; Lei, H. Actual Temperature Evolution of Thick Raft Concrete Foundations and Cracking Risk Analysis. *Adv. Mater. Sci. Eng.* **2019**, *2019*, 7029671. [[CrossRef](#)]
- Bentz, D.; Waller, V.; de Larrard, F. Prediction of Adiabatic Temperature Rise in Conventional and High-Performance Concretes Using a 3-D Microstructural Model. *Cem. Concr. Res.* **1998**, *28*, 285–297. [[CrossRef](#)]
- Statens Byggeforskningsinstitut. *Winter Concreting—Theory and Practice: Proceedings of the RILEM Symposium, Copenhagen, 1956*; SBI forlag: København, Denmark, 1956.
- Schindler, A.K. Effect of Temperature on Hydration of Cementitious Materials. *MJ* **2004**, *101*, 72–81. [[CrossRef](#)]
- Malhotra, V.M. *Maturity Concept and The Estimation of Concrete Strength: A Review*; Department of Mines and Technical Surveys: Ottawa, ON, Canada, 1971.
- Mariak, A. Wyznaczenie wytrzymałości betonu na podstawie funkcji dojrzałości wg amerykańskiej normy ASTM C1074-11. *Constr. Mater.* **2015**, *1*, 70–73. [[CrossRef](#)]
- Zhang, J.; Cusson, D.; Monteiro, P.; Harvey, J. New perspectives on maturity method and approach for high performance concrete applications. *Cem. Concr. Res.* **2008**, *38*, 1438–1446. [[CrossRef](#)]
- Lee, C.; Lee, S.; Nguyen, N. Modeling of Compressive Strength Development of High-Early-Strength-Concrete at Different Curing Temperatures. *Int. J. Concr. Struct. Mater.* **2016**, *10*, 205–219. [[CrossRef](#)]
- Fjellström, P.; Jonasson, J.-E.; Emborg, M.; Hedlund, H. Model for Concrete Strength Development Including Strength Reduction at Elevated Temperatures. *Nord. Concr. Res.* **2012**, *45*, 25–44.

17. CEN. *Eurocode 2: Design of Concrete Structures—Part 1-1: General Rules and Rules for Buildings (EN 1992-1-1:2008)*; British Standards Institution: London, UK, 1992.
18. Saul, A.G.A. Principles underlying the steam curing of concrete at atmospheric pressure. *Mag. Concr. Res.* **1951**, *2*, 127–140. [[CrossRef](#)]
19. Rastrup, E. Heat of hydration in concrete. *Mag. Concr. Res.* **1954**, *6*, 79–92. [[CrossRef](#)]
20. Byfors, J. *Plain Concrete at Early Ages*; Swedish cement and concrete research Institute: Stockholm, Sweden, 1980.
21. Flaga, K. Temperature function of concrete curing at elevated temperatures. Funkcja temperatury betonu tężącego w warunkach podwyższonych temperatur. *Arch. Civ. Eng.* **1969**, *15*, 1–2.
22. Bresson, J.E. Prediction of strength of concrete products. In Proceedings of the RILEM International Conference on Concrete at Early Ages, I. Ecole Nationale des Ponts et Chaussees, Paris, France, 6–8 April 1982; pp. 111–115.
23. Carino, N.J. Maturity functions for concrete. In Proceedings of the RILEM International Conference on Concrete at Early Ages, Paris, France, 6–8 April 1982.
24. Carino, N.J.; Lew, H.S. The Maturity Method: From Theory to Application. In *Structures 2001, Proceedings of the Structures Congress 2001, Washington, DC, USA, 21–23 May 2001*; Chang, P.C., Ed.; American Society of Civil Engineers: Reston, VA, USA, 2012; pp. 1–19. ISBN 978-0-7844-0558-1.
25. Zych, M. Case study of concrete mechanical properties development based on heat temperature measurements. *Cem. Wapno Beton* **2015**, *6*, 383–392.
26. C09 Committee. *Practice for Measuring Hydration Kinetics of Hydraulic Cementitious Mixtures Using Isothermal Calorimetry*; ASTM International: West Conshohocken, PA, USA, 2008.
27. C09 Committee. *Practice for Estimating Concrete Strength by the Maturity Method*; ASTM International: West Conshohocken, PA, USA, 2004.
28. Kurdowski, W.; Pichniarczyk, P. Kłopoty z równaniem Arrheniusa przy ocenie dojrzałości betonu. *Cem. Wapno Beton* **2016**, *21*, 149–156.
29. Roy, D.M.; Cady, P.D.; Sabol, S.A.; Licastro, P.H. *Concrete Microstructure: Recommended Revisions to Test Methods*; National Research Council: Washington, DC, USA, 1993.
30. Kada-Benameur, H.; Wirquin, E.; Duthoit, B. Determination of apparent activation energy of concrete by isothermal calorimetry. *Cem. Concr. Res.* **2000**, *30*, 301–305. [[CrossRef](#)]
31. Kiernożycki, W.; Błyszko, J. Calorimetric measurements and numerical modelling of the effects of selected chemical admixtures on the development of cement hydration at different temperatures. *Cem. Wapno Beton* **2019**, *24*, 432–447. [[CrossRef](#)]
32. Wirquin, E.; Broda, M.; Duthoit, B. Determination of the apparent activation energy of one concrete by calorimetric and mechanical means. *Cem. Concr. Res.* **2002**, *32*, 1207–1213. [[CrossRef](#)]
33. Nielsen, C.V.; Kaasgaard, M. Activation Energy for the Concrete Maturity Model—Part 1: Compressive Strength Tests at Different Curing Temperatures. *Nord. Concr. Res.* **2020**, *62*, 87–106. [[CrossRef](#)]
34. *Methods of Testing Cement. Heat of Hydration. Isothermal Conduction Calorimetry Method*; BS EN 196-11:2018; BSI British Standards: London, UK, 2018.
35. Neville, A.M. *Properties of Concrete*, 5th ed.; Pearson: London, UK, 2012; ISBN 978-0273755807.
36. Regourd, M.; Mortureux, C. Caractérisation et activation thermique des ciments an laitier. In Proceedings of the 7th Congrès International de la Chimie des Ciments, Paris, France, 20 June–4 July 1980; Volume IV.
37. Kurdowski, W. *Chemia Cementu*; Wydawnictwo Naukowe PWN: Warszawa, Poland, 1991; ISBN 9788301103842.
38. Wyrzykowski, M.; Gawin, D. Modelling and experimental study of hydration for ordinary Portland cement. *Archit. Civ. Eng. Environ.* **2010**, *3*, 43–54.
39. Kiernożycki, W. *Betonowe Konstrukcje Masywne: Teoria, Wymiarowanie, Realizacja*; Polski Cement: Kraków, Poland, 2003; ISBN 9788389478009.
40. Wesche, K. Baustoffkennwerte zur Berechnung von Temperaturfeldern in Betonbauteilen. In *Liber Amicorum opgedragen aan F.G. Riessauw ter gelegenheid van zijn zeventigste verjaardag*; RUG Magnel Laboratory for reinforced concrete: Gent, Belgium, 1982.